

## Model for the growth of electrodeposited ferromagnetic aggregates under an in-plane magnetic field

C. Cronemberger,<sup>1,\*</sup> L. C. Sampaio,<sup>1</sup> A. P. Guimarães,<sup>1</sup> and P. Molho<sup>2</sup>  
<sup>1</sup>*CBPF-MCT, Rua Dr Xavier Sigaud, 150, 22290-180 Rio de Janeiro, RJ, Brazil*  
<sup>2</sup>*Institut Néel, CNRS-UJF, BP 166, 38042 Grenoble Cedex 9, France*

(Received 17 August 2009; published 9 February 2010)

The quasi-two-dimensional deposition of ferromagnetic materials by electrochemical process under the influence of a magnetic field applied in the plane of the growth leads to a surprising symmetry breaking in the dendritic structures found. The reasons for these features are still not completely understood. The original dense circular envelope becomes rectangular, as well as the sparse figures have their shapes elongated. This paper reports the results of a diffusion-limited aggregation (DLA) -like simulation. The model proposed here, a modification of the original DLA model, can deal with ferromagnetic particles under the influence of an electric field and the dipolar interactions between particles, submitted to an applied magnetic field in the plane of growth of such structures. The results were produced varying the applied magnetic field and the magnetic moment of the particles and show that the balance between these interactions is an important mechanisms that can be responsible for the changes in shape of the aggregates observed in the experiments.

DOI: [10.1103/PhysRevE.81.021403](https://doi.org/10.1103/PhysRevE.81.021403)

PACS number(s): 61.43.Hv, 82.20.Wt, 68.70.+w

### I. INTRODUCTION

Electrochemical deposition of metals has been intensely studied, since this process can be used in several industrial applications such as microelectronics, magnetic thin film and multilayer deposition [1], and metallic paintings [2], among others. The solidification of metallic alloys is an economically and technically viable technique to produce electronic compounds. Dendritic growth is, for example, one of the failure mechanisms that contribute to the decrease of the lifetime of lithium rechargeable batteries in the cycling of charge [3,4].

Electrodeposition in thin cells gives rise to ramified patterns, with different morphologies depending on parameters like concentration and voltage [5–7]. A magnetic field applied during the deposition may also have strong effects on the morphology [8–13].

Numerical approaches [14–16] have been successfully used to understand the nature of the electrochemical deposits. Reviews of numerical models of fractal growth (and of experiments in different systems) can also be found in the books by Vicsek [17] and Meakin [18]. One example of this is the simulation using a modified Witten and Sander's original *diffusion-limited aggregation* (DLA) model [19,20].

Several modifications of the original DLA model were proposed. One class of modifications of the algorithm is to introduce forces acting on the particle, in competition with thermal fluctuations, thus modifying the rules for the particles motion [15,21,22]. Magnetism was introduced in the numerical models in different ways: attributing a spin to the particles, considering ferromagnetic and antiferromagnetic couplings [23], or studying the aggregation of magnetic microspheres [24]. DLA with long-range dipolar interactions between particles leads to stringy patterns [14], with filaments much less ramified than usual DLA aggregates.

In order to describe the morphologies observed in thin cell electrodeposition under magnetic fields normal to the cell, the DLA algorithm with a rotating flow was able to reproduce the observed chirality induced by the magnetic field [25]. Another method is to introduce the Coulomb forces resulting from the electrical potential and the Lorentz forces induced by the magnetic field applied perpendicular to the plane of the cell [15,22].

In this paper we are interested in an intriguing effect of the magnetic field, observed by Bodea *et al.* [12]. It is a symmetry breaking occurring during electrodeposition in thin cells of ferromagnetic metal (such as Fe or Co), when the magnetic field is applied parallel to the plane of the growth. In experimental conditions that lead to dense circular structures with no magnetic field, a rectangular envelope is observed under magnetic field.

The experiments referred to in the present work were performed in a thin cell, with diameter around 8 cm and thickness smaller than 200  $\mu\text{m}$ . A salt diluted in water (with molar concentrations between  $C=0.06$  M and  $C=0.1$  M) is placed between two electrodes. The internal cathode is a wire in the center of the cell and the external anode is a circular ring, both made of copper. A constant voltage is applied between these electrodes inducing a current. This current is the sum of the currents due to the positive ions moving toward the cathode and the one due to the negative species moving to the external anode. In such conditions, metal deposits at the cathode, producing ramified patterns with a dendritic morphology. Higher concentrations ( $C\sim 0.1$  M) lead to "sparse" aggregates, with few less-ramified branches. Lower concentrations ( $C\sim 0.06$  M) lead to the dense branching morphology (DBM), many thin ramified branches and circular envelope of the aggregate. A magnetic field applied in the plane of growth modifies the morphology: the sparse morphology evolves to thick branches, tending to align with the magnetic field. The DBM morphology becomes less dense (less branches), and a selection of the growth direction of the branches with respect to the magnetic field leads to a rectangular envelope of the aggregate [12].

\*carolina@cbpf.br

Recently, Alves *et al.* [26] published an analysis—using a DLA-like model similar to the one we are using—of the competition between the electric and the dipolar forces in such growth. They have shown that the competition of electric and dipolar interactions can impose some preferential angles to the growth; however the shapes observed in the experiments are not yet mimicked by this model. On their model the thermal fluctuation acts on the magnetic moment of the particle, while on our model it acts on the motion of the particle itself.

This paper presents a numerical simulation based on a modified version of the DLA model, able to reproduce these experimental observations. The model presented here includes the Coulomb force on the ions due to the voltage applied between the electrodes. Each particle bears a magnetic moment, which aligns along the local field, which is the sum of the applied field and the field produced by the particles of the aggregate. The particle motion is then influenced by the magnetic field gradient. The trajectory of the particle is computed, at each step, with a probability that takes into account these forces as described below.

This algorithm is similar to the one used in previous work [22] to simulate electrodeposition under a magnetic field normal to the plane of growth. It has led to a good agreement with experimental results when the fluid motion is neglected. In the present study the fluid motion plays no role, since the magnetic field being in the plane of growth, the Lorentz force would be normal to the cell, and would not induce magnetohydrodynamics convection.

## II. MODEL

One difference between this model and the DLA-like models used to simulate the influence of magnetic fields on the growth of fractal structures [13,21,22,25] is that we used an off-lattice algorithm. The first particle is placed in the center of the lattice. All the others are launched from the rim of the cell (this distance is set to be 2048 units of distance far from the central point). The region where the particles can move on has a periodic boundary condition. At each step the particle has four possibilities for its next position. These positions are located not on a square lattice, but are distributed with a random angle (no longer separated by 90°), on the perimeter of a circle centered on the actual particle position in the same radius  $\delta$  (set in this work as  $\delta=1$  unit of distance). We have noticed that small variations around the value of  $\delta$  do not make a significant change on the shape of the resulting aggregates. This configuration avoids the induction of square patterns from the lattice.

The particles have a diameter of 1 unit of distance. One by one the other particles are launched from an outside circle moving toward the aggregate. The motion of the particle is driven by the potential energy on the region around it. As soon as the particle reaches a position near by the aggregate, it sticks on it. This procedure is repeated until all the  $N$  particles have arrived— $N$  is around 100000.

At each step the particle has four possibilities for its next position. The method sorts the new position based on the probabilities, which are inversely proportional to the poten-

tial energy in each position. Thus, it leads the particle to the region with lower energy.

The motion of each particle is driven by the following.

(1) The Coulombian potential, where  $q_j$  is the charge of the particle  $j$ , which belongs to the aggregate, and  $\kappa$  is the parameter related to the voltage between the electrodes,  $v$ . The voltage has the value  $v=-v_0$  both for the cathode and the aggregate surrounding it, and zero at infinity [27],

$$U_{elect}(\vec{r}_i) = -q_{N+1} \sum_{j=1}^N \frac{u_0}{|\vec{r}_i - \vec{r}_j|}, \quad (1)$$

where  $\vec{r}_i$  is the position of the moving particle and  $\vec{r}_j$  the position of each particle of the aggregate.

(2) The dipolar energy for a particle with magnetic moment  $\mu_i$  in the position  $\vec{r}_i$  is given by

$$U_{mag}(\vec{r}_i) = -\vec{\mu}_i \cdot \vec{B}_T(\vec{r}_i). \quad (2)$$

$B_T$  is the total magnetic field at the particle position given by

$$\vec{B}_T = \vec{B}_{ext} + \sum_{j=1}^N \vec{B}_j \quad (3)$$

$B_T$  is the sum of the external applied constant field,  $\vec{B}_{ext} = B_x \hat{i} + B_y \hat{j}$ , and the magnetic dipolar field,  $\sum_{j=1}^N \vec{B}_j$ , produced by the  $N$  particles of the aggregate. The particle's magnetic moment points always in the direction of the total field at the particle current position,

$$\vec{B}_j(\vec{r}_i) = \frac{\mu_0}{4\pi r^3} \left[ 3 \frac{(\vec{\mu}_j \cdot \vec{r}) \vec{r}}{r^2} - \vec{\mu}_j \right], \quad (4)$$

$\vec{r} = \vec{r}_i - \vec{r}_j$  being the relative position between the moving particle and each particle of the aggregate.

The total energy at the position  $\vec{r}_i$  is given by

$$U(\vec{r}_i) = U_{elect}(\vec{r}_i) + U_{mag}(\vec{r}_i). \quad (5)$$

Differently from the original DLA, the energy difference between the current position and the four possible new positions,  $i=\{1,2,3,4\}$ , ( $\Delta U_i$ ) is used to calculate the probabilities,  $\varphi_i$ , of moving to the new position,  $i$ , given by

$$\varphi_i = \frac{\exp\left(-\frac{1}{k_B T} \Delta U_i\right)}{\sum_i \varphi_i}, \quad (6)$$

where  $k_B T$  is the thermal energy.

Using a Monte Carlo method, one of the four positions is sorted according to their probabilities, and the particle moves to it. At each step, the particle performs its motion guided by these probabilities until it reaches the aggregate and sticks to it. At this point the magnetic moment is fixed in the direction corresponding to the magnetic field in its position and remains with the same orientation until the end of the growth process. With this model, the particles move with higher probability to the region of lower energy.

**III. RESULTS AND DISCUSSION**

The present model has the following control parameters—in arbitrary units: the voltage between the electrodes,  $v$  (set to be  $v=1$  in this paper), the external applied magnetic field  $B$ , the module of the particle’s magnetic moment,  $\mu$ , and the temperature  $T$  ( $k_B T=1/5$  in this paper). In this work we will focus on the influence of the external field,  $B_x$ , varying from 0 to 50, and the magnetic moment of the particle,  $\mu$ , from 0.1 to 10. The influence of  $T$  had been well studied by Alves *et al.* in [26].

Dimensionless parameters will be used. The effective strength of the dipole-dipole interaction ( $d$  is the particle size set to be 1 unit of length) is

$$K_{dd} = \mu^2 / (d^3 k_B T). \tag{7}$$

The effective strength of the dipole-field interaction is

$$K_{df} = \mu B_{ext} / (k_B T). \tag{8}$$

The first group of simulations has been performed with a small particle magnetic moment ( $\mu=0.1$  or  $K_{dd}=0.05$ ) (Fig. 1). The dipole-dipole interaction is small and the resulting aggregates are similar to the ones obtained for nonmagnetic particles [22]. However, for high fields ( $B_x=50$ ,  $K_{df}=25$ ) a change is observed in the magnetic moment orientation. This feature is not strong enough to make an important change in the shape of the aggregate. Nevertheless, the saturation of the magnetization is achieved for high magnetic fields, with all moments pointing parallel to the applied magnetic field, although the shape is not significantly modified [Fig. 1(c)].

A remarkable change appears when the magnetic moment is increased ( $\mu=1$ ,  $K_{dd}=5$ ), as shown in Fig. 2. In this range, the rectangular envelope can be observed even for low values of magnetic field, and the effect becomes more pronounced by increasing the field. For higher fields ( $B_x=50$ ,  $K_{df}=250$ ) the rectangle becomes elongated in the field direction.

The rectangular shape is related to the existence of moments and dipolar interactions. Alves *et al.* [26], only with particles bearing a dipolar momentum and with no magnetic fields, were able to obtain a morphology close to a rectangle. Here, with dipolar momentum and magnetic field, the morphology is very similar to the experiments. The rectangle appears only for intermediate values of  $\mu$ , because a balance between the various energy terms [ $k_B T$ , Coulombian, magnetic field (Zeeman) and dipolar] is necessary: for thermal or Coulombian terms too large, the aggregate remains isotropic and the magnetic effects are negligible. Magnetic moments too large lead to the sparse morphology. Indeed, an impressive effect occurs for aggregates with high value of magnetic moment ( $\mu=10$ ,  $K_{dd}=500$ ) (see Fig. 3). It leads to a very sparse morphology, with few branches, similar to that observed in the experiments for high concentrations of ions in solution [12].

In the case of high  $\mu$ , the dipoles align parallel to each other, forming branches, lines with “magnetic charges” only at the tips. Growth proceeds then more likely from the tips. In the case of intermediate  $\mu$ , dipoles align with the applied field, forming branches with magnetic charges along the

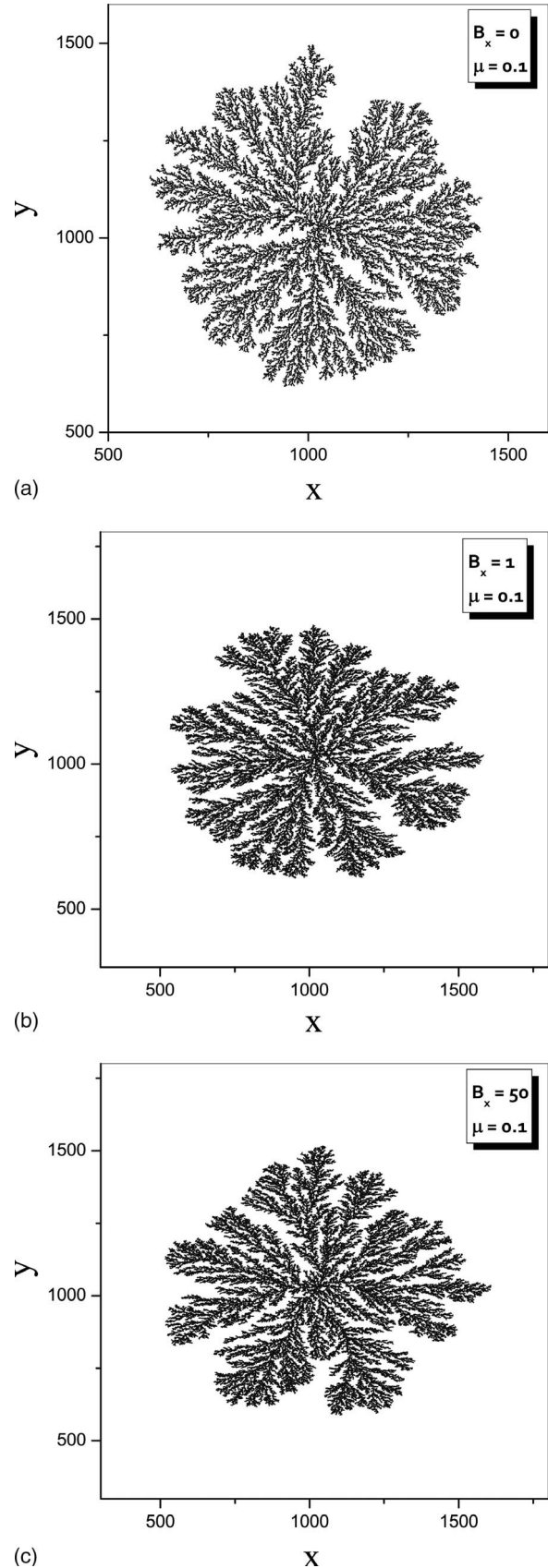
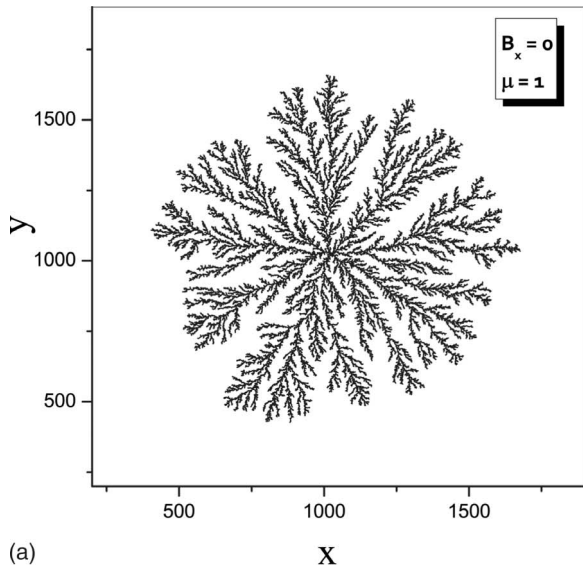
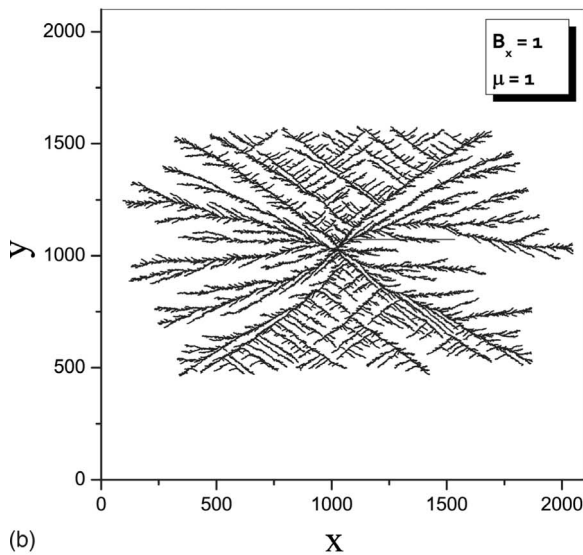


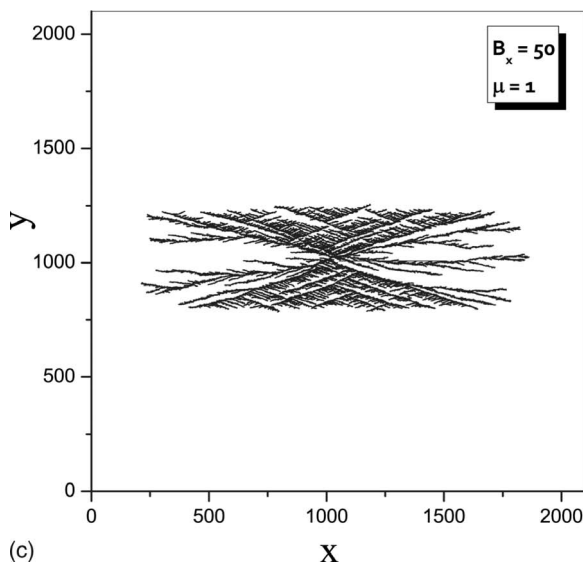
FIG. 1. Aggregates obtained by the simulations for  $v=1$ ,  $\mu=0.1$  and applied magnetic field: (a)  $B_x=0$ , (b)  $B_x=1$ , and (c)  $B_x=50$ .



(a)

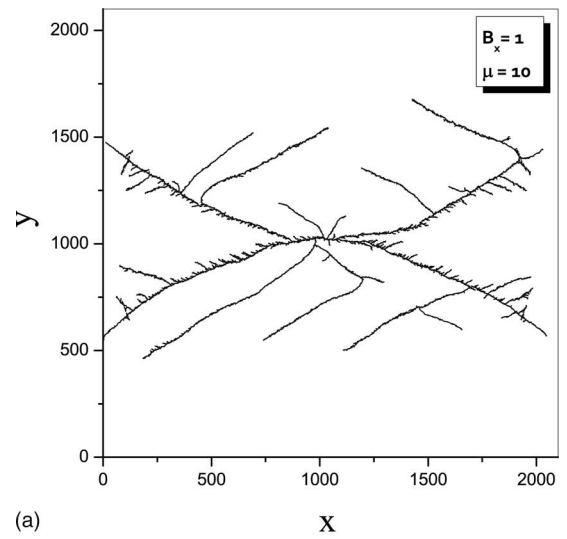


(b)

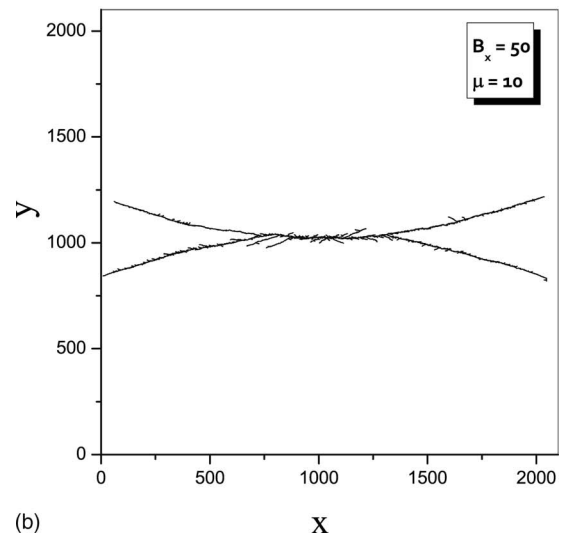


(c)

FIG. 2. Aggregates obtained by the simulations for  $\nu=1$ ,  $\mu=1$  and applied magnetic field: (a)  $B_x=0$ , (b)  $B_x=1$ , and (c)  $B_x=50$ .



(a)



(b)

FIG. 3. Aggregates obtained by the simulations for  $\nu=1$ ,  $\mu=1$ ,  $K_{dd}=500$  and applied magnetic field: (a)  $B_x=1$  and (b)  $B_x=50$ .

lines. The maps of the dipolar part of the energy, shown in Fig. 4, help to visualize the regions with higher probability to be reached. They show regions of lower energy at the tips in the case of high  $\mu$ , therefore a higher probability for the particles to reach the tips, while a uniform distribution of the dipolar energy around the aggregate, in the case of intermediate  $\mu$ .

Another experimental observation concerns the density of the aggregates. Bodea *et al.* [12] reported a reduction of the density of the structures grown under magnetic field, compared with the ones grown with no magnetic field. High density means here high number of branches. Indeed, the fractal dimension  $D_f$  is larger for denser structures and decreases for the sparse ones. Thus,  $D_f$  has been computed for the aggregates using the box counting method (see [17]), and is plotted versus the dimensionless parameter  $K_{dd}$  (Fig. 5). The lower limit of the fractal dimension when  $\mu$  increases,  $D_f = 1.2 \pm 0.1$ , is comparable to the one reported by Pastor-Satorras and Rubi [14], for aggregates grown under the influence of dipolar interactions only, without magnetic field.

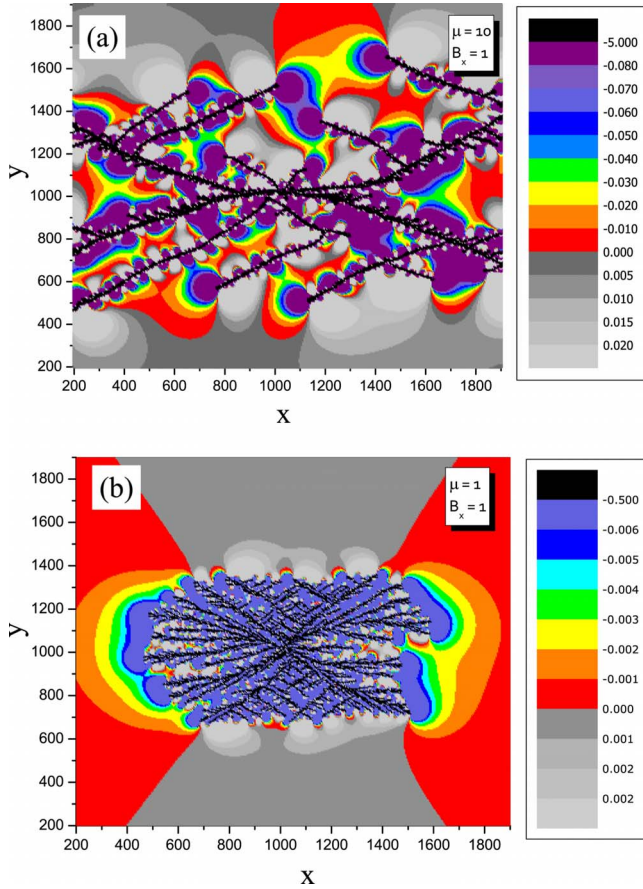


FIG. 4. (Color online) Maps of the dipolar part of the energy  $U^\mu = -\sum_i(B_i \mu)$  on the lattice, for  $B_x=1$  (a)  $\mu=10$  [Fig. 3(a)] and (b)  $\mu=1$  [Fig. 2(b)]. The colors represent the values as shown on the scale at the right.

As already mentioned, increasing the magnetic field elongates the structures in the field direction in both cases, rectangular shape and sparse morphology. In the case of the rectangular shape, this elongation is characterized by mea-

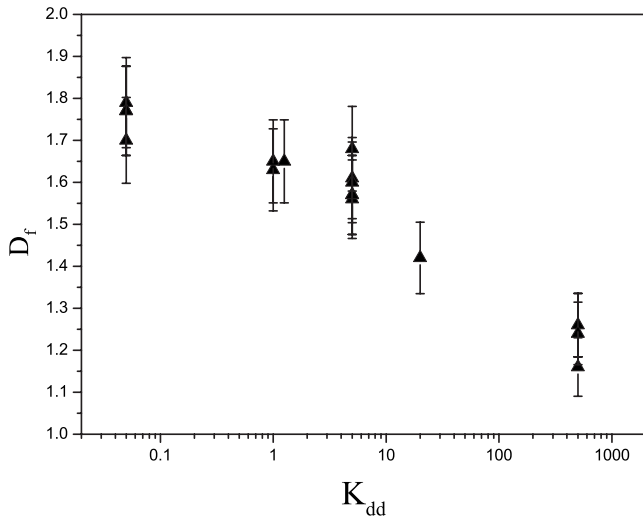


FIG. 5. Fractal dimension  $D_f$  as a function of the dimensionless parameter,  $K_{dd} = \mu^2 / (d^3 k_B T)$ .

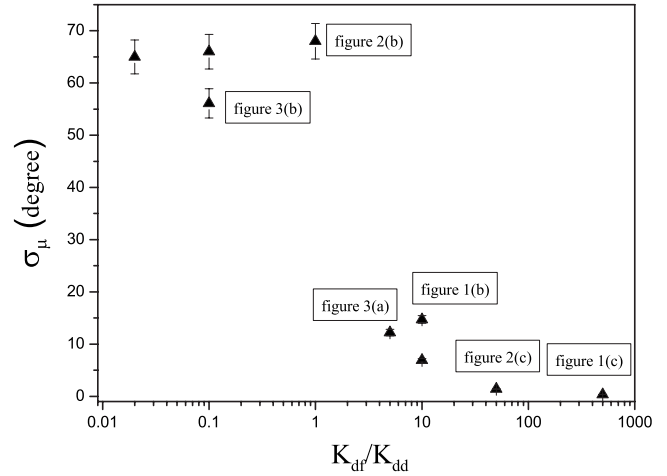


FIG. 6. The dependence of the Gaussian width,  $\sigma$ , fitted from the distribution of the angular orientation of the particles moment, as function of the dimensionless ratio  $K_{df}/K_{dd} = B/\mu$ . The points correspond to the figures indicated by their number.

asuring the angle of the diagonal of the rectangle,  $\theta$ , which decreases when the magnetic field increases. In the case of sparse aggregates, the field aligns the branches in a way similar to magnetic microspheres under magnetic field, like in experiments and simulations reported by Mors *et al.* [28]. They form lines in the field direction; the higher the field, the better the orientation of the lines and of the magnetic dipoles along the field.

When the magnetic moment and the field are large compared to the thermal and Coulombian terms, there is a competition between alignment of the dipoles along the field and along the branches: in high field both orientations may be compatible, when the branches align along the field. The alignment of the magnetic moments can be probed using the distribution of the angle  $\Theta$  between the magnetic moment of the particles and the applied magnetic field. For each aggregate the distribution of  $\Theta$  is a Gaussian centered at  $\Theta=0^\circ$ . The width of the fitting curve,  $\sigma$ , indicates how saturated is each aggregate, small  $\sigma$  meaning that the magnetic moments are well aligned with the magnetic field. The graph of  $\sigma$  as function of the ratio between the field  $B$  and the magnetic moment of the particles is presented in Fig. 6. The number of the figures corresponding to the points of the graph are indicated in order to better associate the images and the degree of alignment with the field. There is a kind of threshold at  $B/\mu$  between 1 and 5. For high values of  $B/\mu$ , the aggregates are elongated, and the saturation of the magnetization can be achieved, while for low values, many branches grow in different directions, allowing for the rectangular shape in case of intermediate values of  $\mu$ .

IV. CONCLUSIONS

In this paper we have shown the results of the simulation performed with a DLA-like model in order to investigate the aggregation of ferromagnetic particles under the influence of the coulomb force and the dipolar interaction, with magnetic field applied in the plane of growth of such structures. These

interactions lead to ramified aggregates both with sparse and dense branching morphologies. We have shown that the effect produced by the field on such structures depends on the amplitude of the magnetic field and the particle magnetic moment.

These simulations are able to reproduce quite well the features observed in the experiments, and give clues to understand the origin of the sparse morphology, the rectangular shape, and the observed field effects. The sparse morphologies obtained with this model arise from a high dipole-dipole interaction. The dipolar field produced by aligned magnetic dipoles induces a stronger force toward the tips. This is the reason why the deposition is more probable at the tips; therefore the structures are less dense (fewer branches) than the one obtained with small magnetic moment.

The rectangular shape is obtained with intermediate values of the dipolar moments. In such case, the balance between the dipole-dipole interaction and the other energy terms (thermal, Coulombian, Zeeman) allow the arriving par-

ticles to deposit with their magnetic moment not only parallel or antiparallel to the orientation of the branches, but in other directions, opening the possibility of new sub-branches, with angles depending on the relative amplitude of each energy term.

There is a competition between alignment of the dipoles parallel to each other, along the branches (high  $\mu$ ), and alignment of the dipoles along the field direction (high field). When the magnetic field is increased, the dipoles become better aligned along the field (therefore the saturation of the magnetization is increased) and the aggregates become elongated in the direction of the magnetic field, both for the rectangular shapes and the sparse morphology.

#### ACKNOWLEDGMENTS

The authors thank the CAT/CBPF for the use of the SSOLAR cluster computer facility. The work is supported by CNPq, Brazil.

- 
- [1] V. Fleury, W. A. Watters, L. Allam, and T. Devers, *Nature* (London) **416**, 716 (2002).
- [2] P. Olivas, Ph.D. thesis, Institut National Polytechnique de Grenoble (2001).
- [3] J. M. Tarascon and M. Armand, *Nature* (London) **414**, 359 (2001).
- [4] C. Monroe and J. Newman, *J. Electrochem. Soc.* **150**, A1377 (2003).
- [5] Y. Sawada, A. Dougherty, and J. P. Gollub, *Phys. Rev. Lett.* **56**, 1260 (1986).
- [6] M. Matsushita, M. Sano, Y. Hayakawa, H. Honjo, and Y. Sawada, *Phys. Rev. Lett.* **53**, 286 (1984).
- [7] D. Grier, E. Ben-Jacob, R. Clarke, and L. M. Sander, *Phys. Rev. Lett.* **56**, 1264 (1986).
- [8] I. Mogi, M. Kamiko, S. Okubo, and G. Kido, *Physica B* **201**, 606 (1994).
- [9] I. Mogi, M. Kamiko, and S. Okubo, *Physica B* **211**, 319 (1995).
- [10] J. M. D. Coey, G. Hinds, and M. E. G. Lyons, *Europhys. Lett.* **47**, 267 (1999).
- [11] S. Bodea, L. Vignon, R. Ballou, and P. Molho, *Phys. Rev. Lett.* **83**, 2612 (1999).
- [12] S. Bodea, R. Ballou, and P. Molho, *Phys. Rev. E* **69**, 021605 (2004).
- [13] T. R. Ni Mhócháin, G. Hinds, A. Martin, E. Chang, A. Lai, L. Costiner, and J. M. D. Coey, *Electrochim. Acta* **49**, 4813 (2004).
- [14] R. Pastor-Satorras and J. M. Rubí, *Phys. Rev. E* **51**, 5994 (1995).
- [15] V. A. Bogoyavlenskiy, *J. Phys. A* **35**, 2533 (2002).
- [16] T. R. Ni Mhócháin and J. M. D. Coey, *Phys. Rev. E* **69**, 061404 (2004).
- [17] T. Vicsek, *Fractal Growth Phenomena*, 2nd ed. (World Scientific, Singapore, 1992).
- [18] P. Meakin, *Fractals, Scaling and Growth Far From Equilibrium* (Cambridge University Press, Cambridge, 1998).
- [19] T. A. Witten and L. M. Sander, *Phys. Rev. Lett.* **47**, 1400 (1981).
- [20] T. A. Witten and L. M. Sander, *Phys. Rev. B* **27**, 5686 (1983).
- [21] S. G. Alves and S. C. Ferreira, Jr., *J. Phys. A* **39**, 2843 (2006).
- [22] C. M. Cronemberger and L. C. Sampaio, *Phys. Rev. E* **73**, 041403 (2006).
- [23] N. Vandewalle and M. Ausloos, *Phys. Rev. E* **51**, 597 (1995).
- [24] G. Helgesen, A. T. Skjeltorp, P. M. Mors, R. Botet, and R. Jullien, *Phys. Rev. Lett.* **61**, 1736 (1988).
- [25] N. Nagatani and F. Sagues, *J. Phys. Soc. Jpn.* **59**, 3447 (1990).
- [26] S. G. Alves, F. L. Braga, and M. L. Martins, *J. Stat. Mech.* (2007), P10015.
- [27] J. D. Jackson, *Classical Electrodynamics*, 3rd ed. (Wiley, New York, 1998).
- [28] P. M. Mors, R. Bolet, and R. Jullien, *J. Phys. A* **20**, L975 (1987).